Supporting information

Manipulating Electron Redistribution in Platinum for Enhanced Alkaline Water Splitting Kinetics

Wensheng Zhang, Xu Chen, Jinyu Zhao, Lin Niu, Guipeng Wang, Xiaomin Wang*

College of Materials Science and Engineering, Taiyuan University of Technology, 030024, PR China

E-mail address: wangxiaomin@tyut.edu.cn (X.Wang)

Material Characterization

The crystal structure of the irradiated samples was investigated using X-ray diffraction (XRD, Smart Lab) measurements, employing Cu Kα radiation in a 2θ range from 5 to 80°. The surface morphology and elemental composition were analyzed using a scanning electron microscope (SEM, Zeiss Gemini 300) equipped with an energy dispersive spectrometer (EDS). Transmission electron microscopy (TEM) images were acquired using a JEOL JEM 2100F. To examine the chemical composition of the surface of the synthesized materials, X-ray photoelectron spectroscopy (XPS) analyses were conducted on a Thermo Fisher instrument utilizing an Al Kα radiation source. Additionally, the platinum content in the samples was quantified using an inductively coupled plasma optical emission spectrometer (ICP-OES, PerkinElmer 8300).

Electrochemical measurement

Electrochemical tests were conducted using a CHI 760E electrochemical

workstation (Shanghai Chenhua Instrument Co.) in a standard three-electrode system in 1M KOH. The prepared catalyst (2cm x 1cm) served as the working electrode, with a graphite rod and Ag/AgCl electrode acting as the counter electrode and reference electrode for OER and HER activity, respectively. A dual-electrode system using the prepared catalyst was employed in 1.0M KOH to investigate overall water splitting performance, functioning as both anode and cathode. All potentials in the tests were calibrated to the Reversible Hydrogen Electrode (RHE) scale using the Nernst equation: $E(RHE) = E(Ag/AgCl) + 0.197 + 0.0591 \times pH$, where $\eta = E(RHE) - 1.23V$. All Linear Sweep Voltammetry (LSV) measurements were conducted at a scan rate of 5 mV s^{-1}, with HER and OER performed in the ranges of -1.5 ~ -1V and 0 ~ 1V (vs. Ag/AgCl) respectively, applying 90% iR correction. Prior to LSV measurements, 40 cycles of Cyclic Voltammetry (CV) were performed to enhance the catalyst's activity and stability. Tafel plots were obtained by fitting the polarization curves between overpotential (η) and logarithmic current density (log j) using the equation: $\eta = b\ log(j) + a$, where b is the Tafel slope. For HER and OER, CV curves were recorded in the potential ranges of -0.74 ~ -0.64 V and 0.1 ~ 0.2 V (vs. Ag/AgCl), respectively, at scan rates of 20 ~ 40 mV s^{-1}. Double-layer capacitance (C_{dl}) values were calculated based on the CV curves in the non-Faradaic potential region. Electrochemical active surface area (ECSA) was calculated using the formula: $ECSA = C_{dl}/Cs$, where Cs is the specific capacitance of a flat surface, taken as 0.040 mF cm^{-2} in 1M KOH. Electrochemical Impedance Spectroscopy (EIS) was obtained at a potential of 0.5 V, with a test frequency range of 10^{-2} ~ 10^{5} Hz and an AC voltage of 5 mV. Long-term

durability tests were assessed using chronoamperometry at a current density of 100 mA cm^{-2}.

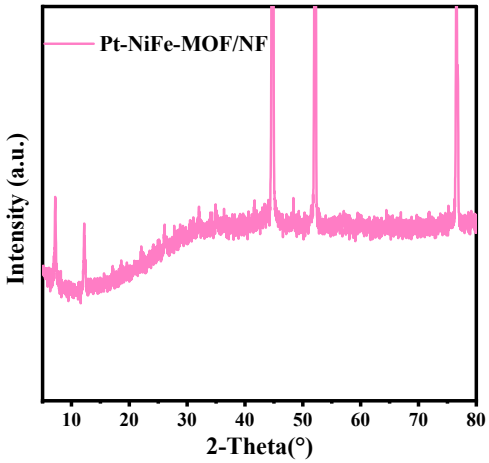

Figure S1. Enlarged XRD spectrum of Pt-NiFe-MOF.

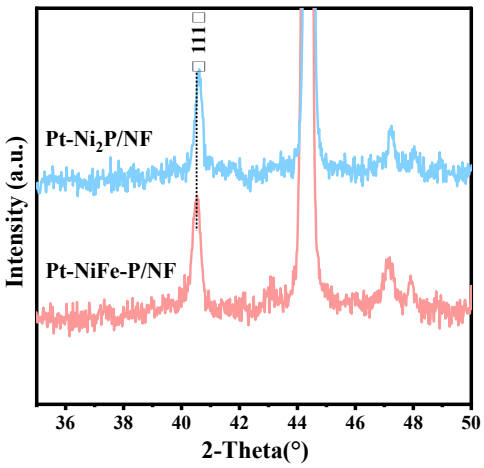

Figure S2. Enlarged XRD spectra of Pt-NiFe-P/NF and Pt-Ni_2P/NF.

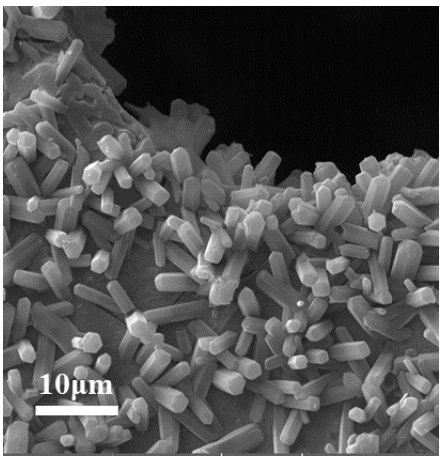

Figure S3. SEM image of Pt-NiFe-P/NF.

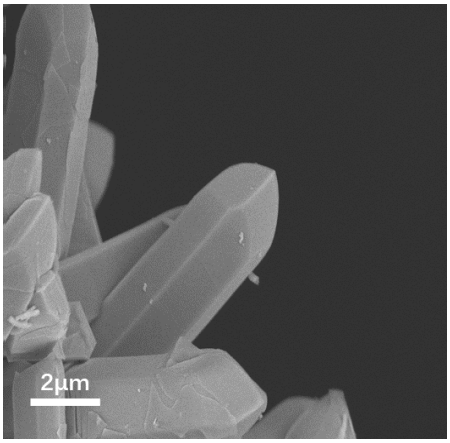

Figure S4. Enlarged SEM image of NiFe-P/NF.

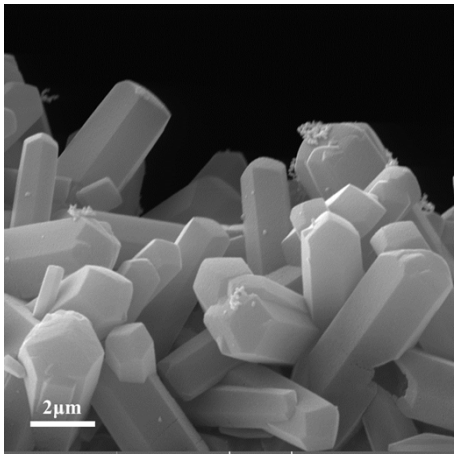

Figure S5. Enlarged SEM image of NiFe-MOF/NF.

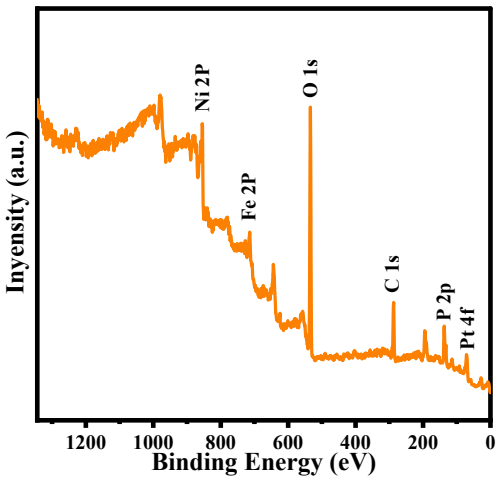

Figure S6. The XPS survey spectrum of Pt-NiFe-P/NF.

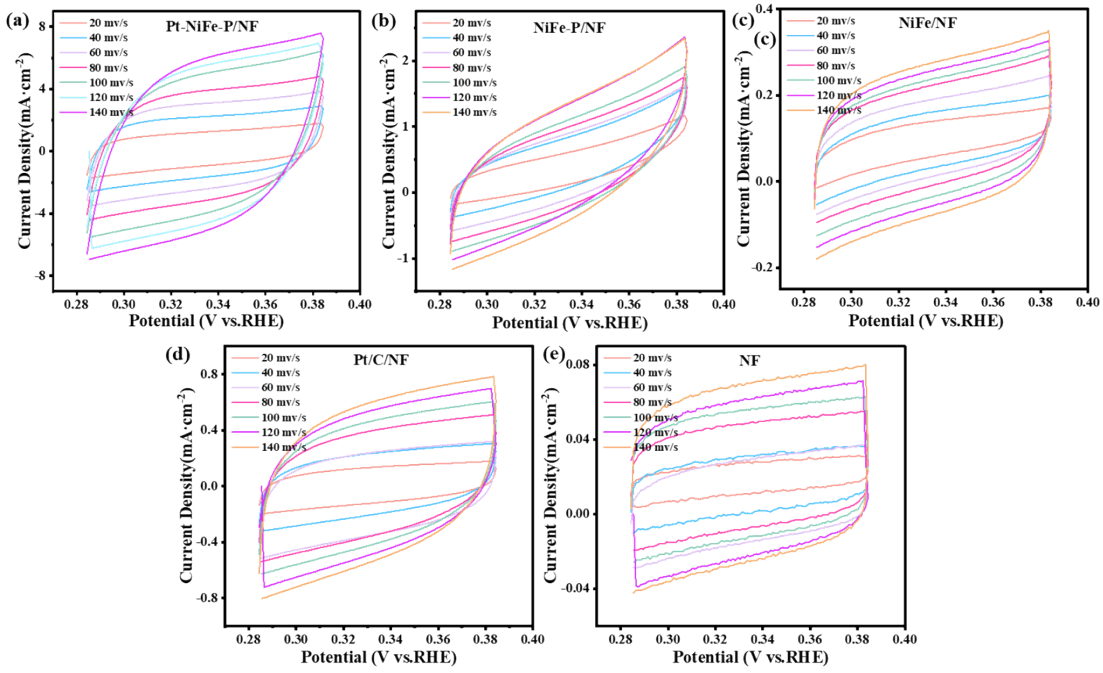

Figure S7. Cyclic voltammetry curves for HER testing in 1M KOH aqueous solution at different scan rates for (a) Pt-NiFe-P/NF. (b) NiFe-P/NF. (c) NiFe-MOF/NF. (d) Pt/C/NF. and (e) NF.

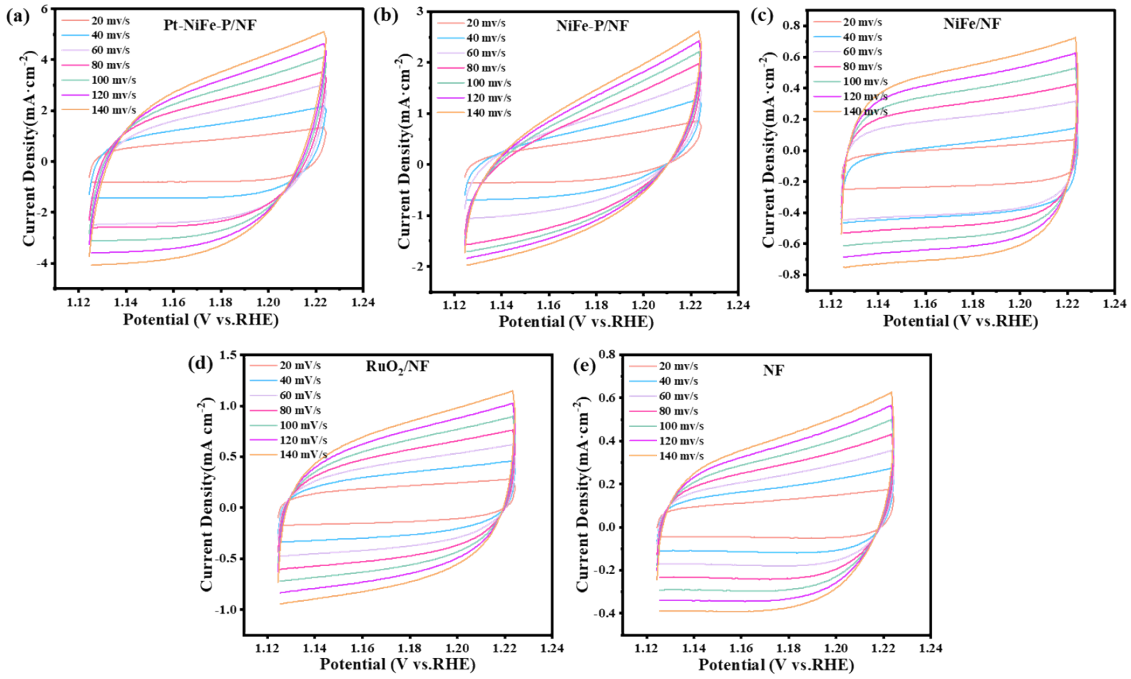

Figure S8. Cyclic voltammetry curves for OER testing in 1M KOH aqueous solution at different scan rates for (a) Pt-NiFe-P/NF. (b) NiFe-P/NF. (c) NiFe-MOF/NF. (d) RuO_2/NF. (e) NF.

Table S1. Comparison of HER and OER performance of Pt-NiFe-P/NF with other reported self-supported highly active HER and OER electrocatalysts in 1 M KOH.

Catalysts	Overpotential@10 mA cm^{-2}	Overpotential@100 mA cm^{-2}	Electroyte	References
	HER	OER		
Pt-NiFe-P/NF	17	266	1 M KOH	This work
Ru-NiCoP/NF	44	285	1 M KOH	[1]
Ni_2P/CoP-Pt	44.2	-	1 M KOH	[2]
Ru-CoFe@C/NF-HR	-	257	1 M KOH	[3]
Pt_{SA}-Ni_2P@NF	26	-	1 M KOH	[4]
Pt-B-NiFe-LDH	19	229	1 M KOH	[5]
Pt-NiFe LDH	36	226	1 M KOH	[6]
Ru-(Ni/Fe)C_2O_4	42	-	1 M KOH	[7]
Ru-NiFeP/NF	29.3	227	1 M KOH	[8]
Pt_{SA}-NiO/Ni	26	-	1 M KOH	[9]
Pt-Ni$(OH)_x$	58	-	1 M KOH	[10]
Ir–NiCo LDH	21	245	1 M KOH	[11]
Pt–CoFe(II)	21	239	1 M KOH	[12]

Table S2. Comparison of water splitting performance of Pt-NiFe-P/NF with other reported highly active bifunctional electrocatalysts in 1 M KOH.

Catalysts	Potential@10 mA cm^{-2}	Electroyte	References
Pt-NiFe-P/NF	1.45 V	1 M KOH	This work
Pt@CoS_2-NrGO	1.48 V	1 M KOH	[13]
Co-$ZnRuO_x$	1.48 V	1 M KOH	[14]
Ir_{NPs}/NiCo LDH	1.45 V	1 M KOH	[15]
Pt–CoFe(II) LDH	1.511 V	1 M KOH	[16]
Ru-NiFeP/NF	1.47 V	1 M KOH	[17]
Pt/NiFeV	1.54 V	1 M KOH	[18]
Ru-NiCoP/NF	1.515 V	1 M KOH	[19]
Pt/Ni_xFe LDHs	1.47 V	1 M KOH	[20]
Pt-$NiMoO_4$-GO/NF	1.515 V	1 M KOH	[21]

1 D. Chen, R. Lu, Z. Pu, J. Zhu, H.-W. Li, F. Liu, S. Hu, X. Luo, J. Wu, Y. Zhao and S. Mu, *Appl Catal B-environ*, 2020, **279**, 119396.
2 Y. Tan, J. Feng, H. Dong, L. Liu, S. Zhao, F. Lai, T. Liu, Y. Bai, I. P. Parkin and G. He, *Adv Funct Mater*, 2023, **33**, 2209967.
3 J. Ren, J. Liu, Y. Du, S. Li, M. Wang, B. Li, B. Yang, L. Wang and Y. Liu, *Nano Res*, 2023, **16**, 10810–10821.
4 D. Ren, G. Wang, L. Li, Y. Jin, K. Zhou, C. Zeng, Q. Zhang, J. Liu, R. Wang, X. Ke, M. Sui and H. Wang, *Chem Eng J*, 2023, **454**, 140557.
5 L. Tan, H. Wang, C. Qi, X. Peng, X. Pan, X. Wu, Z. Wang, L. Ye, Q. Xiao, W. Luo, H. Gao, W. Hou, X. Li and T. Zhan, *Appl Catal B-environ*, 2024, **342**, 123352.
6 X. He, X. Han, X. Zhou, J. Chen, J. Wang, Y. Chen, L. Yu, N. Zhang, J. Li, S. Wang and H. Jin, *Appl Catal B-environ*, 2023, **331**, 122683.
7 J. Zhao, H. Guo, Q. Zhang, Y. Li, L. Gu and R. Song, *Appl Catal B-environ*, 2023, **325**, 122354.
8 Y. Lin, M. Zhang, L. Zhao, L. Wang, D. Cao and Y. Gong, *Appl Surf Sci*, 2021, **536**, 147952.
9 K. L. Zhou, Z. Wang, C. B. Han, X. Ke, C. Wang, Y. Jin, Q. Zhang, J. Liu, H. Wang and H. Yan, *Nat Commun*, 2021, **12**, 3783.
10 Q. Li, Q. Zhang, W. Xu, R. Zhao, M. Jiang, Y. Gao, W. Zhong, K. Chen, Y. Chen, X. Li and N. Yang, *Adv Energy Mater*, 2023, **13**, 2203955.
11 R. Fan, Q. Mu, Z. Wei, Y. Peng and M. Shen, *J Mater Chem A*, 2020, **8**, 9871–9881.
12 J. Wu, Z. Nie, R. Xie, X. Hu, Y. Yu and N. Yang, *J Power Sources*, 2022, **532**, 231353.
13 N. Logeshwaran, S. Ramakrishnan, S. S. Chandrasekaran, M. Vinothkannan, A. R. Kim, S. Sengodan, D. B. Velusamy, P. Varadhan, J.-H. He and D. J. Yoo, *Appl Catal B-environ*, 2021, **297**, 120405.
14 D. Liu, Z. Wu, J. Liu, H. Gu, Y. Li, X. Li, S. Liu, S. Liu and J. Zhang, *Small*, 2023, **19**, 2207235.
15 R. Fan, Q. Mu, Z. Wei, Y. Peng and M. Shen, *J Mater Chem A*, 2020, **8**, 9871–9881.
16 J. Wu, Z. Nie, R. Xie, X. Hu, Y. Yu and N. Yang, *J Power Sources*, 2022, **532**, 231353.
17 Y. Lin, M. Zhang, L. Zhao, L. Wang, D. Cao and Y. Gong, *Appl Surf Sci*, 2021, **536**, 147952.
18 Y. Feng, Z. Li, S. Li, M. Yang, R. Ma and J. Wang, *J Energy Chem*, 2022, **66**, 493–501.
19 D. Chen, R. Lu, Z. Pu, J. Zhu, H.-W. Li, F. Liu, S. Hu, X. Luo, J. Wu, Y. Zhao and S. Mu, *Appl Catal B-environ*, 2020, **279**, 119396.
20 X. Yu, J. Guo, B. Li, J. Xu, P. Gao, K. S. Hui, K. N. Hui and H. Shao, *Acs Appl Mater Inter*, 2021, **13**, 26891–26903.
21 X. Deng, J. Chen, C. Zhang, Y. Yan, B. Wu, J. Zhang, G. Wang, R. Wang and J. Chen, *J Colloid Interf Sci*, 2023, **640**, 928–939.